Quantum radiation of a harmonic oscillator near the planar dielectric-vacuum interface

Maciej Janowicz
Institute of Physics, Nicholas Copernicus University, Grudziądzka 5, Toruń 87-100, Poland

Władysław Żakowicz
Institute of Physics, Polish Academy of Sciences, Al.Lotników 32, Warsaw 02-668, Poland
(Received 13 July 1993)

A harmonic oscillator interacting with the electromagnetic field in the vicinity of the planar dielectric-vacuum interface has been analyzed. The electromagnetic field is described in terms of Carniglia-Mandel modes (triple-wave modes) which take into account proper boundary conditions at the interface. Exact resolvent functions, which determine the solution of the initial-value problem for the oscillator and the electromagnetic field, have been obtained. These functions give frequency shifts and decay times for oscillator excitations. In most cases, when the oscillator approaches the interface, its excitation decay time decreases. Radiative frequency shifts have been calculated and interpreted in terms of the coupling with the Carniglia-Mandel photons. Outgoing photons, i.e., photons characterized by the outgoing waves and the outgoing wave vectors, have been used for a description of angular radiation intensity patterns. Some results for the radiative damping and the radiation angular distribution are equivalent to the classical ones, however, they get a new quantum interpretation.

PACS number(s): 42.50.−p, 32.80.−t, 12.20.Ds

I. INTRODUCTION

There is much current interest in modifications of atomic radiative processes due to changes of the environment. Originally, effects such as spontaneous emission, radiative decay, and radiative frequency shifts were considered in the empty space with corresponding structure of the free electromagnetic field. Various optical elements, e.g., mirrors, resonators, or simply optically active media, cause changes in the properties of the free electromagnetic field. The modifications of the free field affect all atomic radiative processes.

Historically, the first radiation emission problem in which the environment played a crucial role was analyzed by Sommerfeld, who studied the emission and wave propagation of radio wave antennas [1,2]. Dielectric and conductive properties of the Earth surface were crucial for his study. Investigating various dipole antennas, Sommerfeld described the field emitted by those antennas and gave formulas for energy losses (radiative damping constant of the oscillating dipole); in fact, he found the Green function for the Helmholtz wave equation such that the continuity conditions on the boundary plane between air and Earth were automatically fulfilled. The problem of asymptotic properties of Sommerfeld's solution has attracted a lot of attention in the past few decades [3,4].

Similar modifications of radiative properties due to changes of the environment, resulting in modifications of the free electromagnetic field, were expected for microscopic atomic sources. In 1946 Purcell [5] pointed out that the spontaneous emission rate should increase significantly when the radiation is held in a lossy resonant LC circuit. This circuit plays the role of a resonant cavity in current optical experiments. With recent technological progress a construction of microscopic resonant cavities and waveguides has become feasible. In these structures the atomic radiative decay as well as the frequency shifts can be measured. Excited atoms can exhibit either enhanced or suppressed radiative decay. Interaction of atoms with the electromagnetic field inside optical resonators and optical waveguides ia subject of the so called cavity quantum electrodynamics (CQED) [6].

The first experiment in the optical region in which atomic radiative processes have been modified by the environment was done by Drexhage (and co-workers) in 1968 [7–9] who measured the lifetime and frequency shift of some molecules near a metallic surface. Apart from the increase of frequency by several orders of magnitude these systems resemble very much those investigated originally by Sommerfeld. Not surprisingly, Drexhage's results on the decay rate were theoretically explained by Morawitz [10], Morawitz and Philpott [11], and Chance, Prock, and Silbey [12] using the classical Sommerfeld approach.

Analyses of the frequency shift of atoms in the vicinity of dielectrics and imperfect conductors have also been presented (for small values of the distance from the conducting medium) by Chance and co-workers [13] (see Ref. [14] for more references). Recently, this type of frequency shift in a micrometer-sized cavity has been measured by Sandoghar *et al.* [15].

The above investigations were based mainly on classical electrodynamics. In the present paper we want to discuss a similar system, an atom modeled by a harmonic oscillator, placed in the vicinity of a planar boundary of a dielectric occupying the half space. Our discussion is based on the quantum electrodynamical approach.

The quantum approaches were also applied in previous analyses of similar systems. Particular problems have

been treated in [16–26]. These papers cover, within some approximations, various aspects of the interaction of atoms with the electromagnetic field in different environments, e.g., spontaneous emission rates and frequency shifts [19,20].

Modifications of atomic processes occur also for atoms immersed inside a homogeneous dielectric. Glauber and Lewenstein [27] presented a general scheme of quantization of the electromagnetic field in a linear and nondispersive dielectric medium. They also obtained the spontaneous emission rate of an atom embedded in an infinite uniform dielectric, taking into account local field effects. Corresponding expressions for the decay rate were independently derived and checked experimentally by Yablonovich *et al.* [28].

The relative simplicity of a harmonic oscillator interacting with the electromagnetic field corresponding to the imposed environment configuration permits an almost exact solution of its quantum dynamics. The procedure leading to this solution illustrates the detailed structure of coupling between electromagnetic field modes and sources. This may help in treating more complicated systems, e.g., dielectric resonators and waveguides.

Our approach follows the works [29,30] on harmonic oscillators interacting with an electromagnetic field in vacuum. However, we have to modify the description of the free electromagnetic field according to the implemented structure of space. In our case the half space is occupied by transparent dielectric with a planar boundary while the second half space is empty. The oscillator can be located either in the vacuum side or inside the dielectric.

Very useful in the description of the interaction of radiating systems with the electromagnetic field and a dielectric half space with a planar boundary was construction of a mode decomposition of the field given by Carniglia and Mandel (CM modes) [34]. Their modes automatically take into account the boundary conditions. The modes are orthonormal and, as has been proved in [35], form a complete set. The CM modes and the corresponding photons that can be connected with these modes are the key ingredient of our analysis.

One of the important properties of radiation emission near the dielectric interface is its directional intensity characteristics. For Sommerfeld and many of his followers the knowledge of the radiation patterns had very important and practical applications in the construction of efficient directional antennas. For atomic microsources the angular intensity distributions were described and experimentally investigated in [31]. It was theoretically predicted and experimentally observed that for a source near the dielectric boundary much of the radiation is emitted into the dielectric at angles around the critical angle for a total internal reflection. Similar properties are stated in [32].

Previous discussions of directional properties of the spontaneous emission of atoms were given almost exclusively in terms of the classical electrodynamics. In our paper we want to discuss a directional emission pattern in the framework of quantum electrodynamics and the modes and photons introduced by Carniglia and Mandel. There was some ambiguity about how these CM photons, associated with triple waves (incoming, reflected, and transmitted), can determine the emission directional characteristics. An attempt [27] to apply those photons to the description of a transition radiation, emitted when an electron crosses the boundary between two dielectrics, is not correct. The quantum interference effect between two paths, corresponding to two kinds of CM photon emission, was overlooked [33]. The above difficulties can be avoided if one introduces, equivalent to the CM modes, the set of modes which are parametrized by the outgoing waves. The original Carniglia-Mandel modes are parametrized by the incoming waves.

Although the exact dynamics of the system composed of a harmonic oscillator coupled to an electromagnetic field is found in this paper, our description of the radiation intensity pattern will be based on a standard perturbation theory approach. Thus we will not be able to describe temporal and spectral characteristics of the emitted radiation. However, a photonic interpretation of the angular intensity pattern will be simpler.

While our discussion solves a harmonic oscillator problem, i.e., the problem of the simplest possible radiation source, not all results derived here may be valid for real atoms which are basically nonlinear objects with a complex structure of energy levels and resonances. Nevertheless, we may expect that our discussion provides a useful qualitative insight into the modifications of atomic radiative processes by environmental changes and related changes of the free electromagnetic field. We may expect quantitative validity of our results in situations when a system of real atoms is well approximated by harmonic oscillators. Generally that occurs for weakly excited systems. Besides, a harmonic oscillator model is adequate for the description of nonrelativistic electrons in a static uniform magnetic field. Their interaction with the electromagnetic field in the free space given in [36] can be extended, using our approach, to more complex situations, e.g., electrons inside semiconductors, close to a boundary, in uniform magnetic field. This application of our approach will be addressed in future work.

The rest of the paper is organized as follows. In Sec. II we formulate and solve equations describing the dynamics of a system composed of an oscillator and electromagnetic field. The oscillator can be located either outside or inside the dielectric half space. The resolvent functions contain information on radiative decay lifetimes and radiative frequency shifts. In a particular case, i.e., when the oscillator is placed outside the dielectric, the computed decay time agrees with that previously derived by Sommerfeld and Morawitz by different methods. The decay time of an oscillator located in a dielectric and far from the interface agrees with the decay time derived in [28,27] for an atom embedded in a dielectric. In Sec. III we discuss the angular intensity distribution of the oscillator's radiation. Section IV contains some concluding remarks. In Appendix A 1 we recall the Carniglia-Mandel modes following their definitions given in [34], while in Appendix A 2 we define an equivalent set of outgoing modes, useful in discussions of the directional emission pattern.

II. DYNAMICS OF CHARGED HARMONIC OSCILLATOR NEAR THE DIELECTRIC-VACUUM INTERFACE

Let us consider a harmonic oscillator, located at a point $\mathbf{r}_0=(0,0,h)$ near the dielectric-vacuum interface. An ideal, homogeneous, lossless, and nondispersive dielectric, with the refraction index n, is occupying the left half space, Fig. 1. The oscillator is composed of a charge e, having a mass m, bound to a fixed center by the elastic force. We are interested in the charge dynamics due to its interaction with the electromagnetic field. We will use the dipole approximation and choose a system of units with $\hbar=c=1$.

The Hamiltonian of the system, written in the Coulomb gauge, $\mathrm{div}(\epsilon\mathbf{A})=0$, is

$$H=\frac{1}{2m}[\mathbf{p}-e\eta\mathbf{A}(\mathbf{r}_0)]^2+\tfrac{1}{2}m\omega_0^2\mathbf{x}^2+V_{d\text{-}v}^{\mathbf{r}_0}(\mathbf{x})+H_F\ , \tag{1}$$

where the free field Hamiltonian, expressed in terms of the V and D photons described in Appendix A, is

$$H_F=\frac{1}{(2\pi)^3}\sum_{s=1,2}\left[\int_{K_3<0}d_3\mathbf{K}\,K a_{K,s}^{\dagger\mathrm{V}}a_{K,s}^{\mathrm{V}}+\int_{k_3>0}d_3\mathbf{k}\,K a_{k,s}^{\dagger\mathrm{D}}a_{k,s}^{\mathrm{D}}\right] \tag{2}$$

and $V_{d\text{-}v}$ is the instantaneous electrostatic dipole-dielectric interaction necessary in the Coulomb gauge. It is equal to

$$V_{d\text{-}v}^{\mathbf{r}_0}(\mathbf{x})=\tfrac{1}{2}m\mathbf{x}^T\cdot\hat{\mathbf{D}}_{\hat{e}}\cdot\mathbf{x}\ , \tag{3}$$

where

$$\hat{\mathbf{D}}_e=-\frac{e^2}{4\pi\epsilon_0 m}\frac{1}{(2h)^3}\frac{n^2-1}{n^2+1}\hat{\mathbf{V}}_0 \tag{4}$$

if the oscillator is placed in the vacuum ($h>0$) and

$$\hat{\mathbf{D}}_e=\hat{\mathbf{D}}_e^{\mathrm{diel}}=\frac{\eta^2e^2}{4\pi\epsilon_0 mn^2}\frac{1}{(2|h|)^3}\frac{n^2-1}{n^2+1}\hat{\mathbf{V}}_0 \tag{5}$$

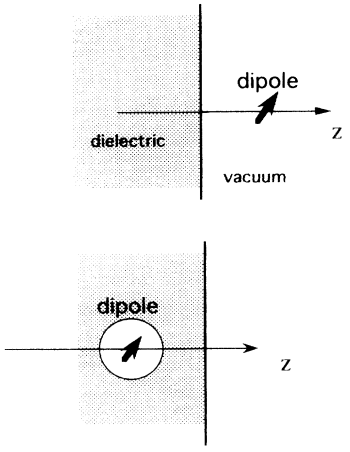

FIG. 1. Oscillator near dielectric-vacuum interface. The oscillator in a dielectric is placed in a microscopic spherical vacuum hole.

if it is located in the dielectric ($h<0$). The matrix $\hat{\mathbf{V}}_0$ is

$$\hat{\mathbf{V}}_0=\begin{bmatrix}1&0&0\\0&1&0\\0&0&2\end{bmatrix}\ . \tag{6}$$

The factor parameter η is supposed to imitate local near field effects in the dielectric, similar to those included in the derivation of the Clausius-Mossotti law. It indicates a distinction between the macroscopic mean field in the dielectric and the microscopic field which actually couples to the dipole. The η factor can be obtained in a model in which the radiating atom is placed in the center of a small spherical hole inside the dielectric. In this case

$$\eta=\frac{3n^2}{2n^2+1}\ . \tag{7}$$

The electron displacement from its equilibrium position is $\mathbf{x}$ and its canonical momentum is $\mathbf{p}$. The vector potential taken at the position of the center of the oscillator is basically given by Eq. (A8) of Appendix A. However, high-frequency cutoff functions $g_n(K)$ replacing $1/\sqrt{K}$ have to be introduced to make the model finite within the dipole approximation. Similarly as in [29] the following cutoff form factor is used:

$$g_n(K)=\frac{1}{\sqrt{K}}\frac{\Omega_n}{\sqrt{\Omega_n^2+K^2}}\ . \tag{8}$$

The index n indicates a distinction in the frequency cutoff function for an oscillator placed in the vacuum and one placed in the dielectric. The cutoff form factor tempers the waves violating the dipole approximation. As the waves of a given frequency are shorter in the dielectric, the corresponding cutoff frequency Ω_n should be reduced. It seems reasonable to take $\Omega_n=\Omega_{\mathrm{vac}}/n$. In such a case there is only one cutoff function when it is expressed in terms of the length of the wave vector.

The dynamics of the system, i.e., the oscillator and the field, is determined by the Heisenberg equations of motion for the complete set of dynamical variables. This complete set includes the electron position and velocity $\mathbf{x}$, $\mathbf{v}=(1/m)[\mathbf{p}-e\eta\mathbf{A}(\mathbf{r}_0)]$, and the photon creation and annihilation operators $a_{\mathbf{K},s}^{\mathrm{V}}$, $a_{\mathbf{K},s}^{\dagger\mathrm{V}}$, $a_{\mathbf{k},s}^{\mathrm{D}}$, $a_{\mathbf{k},s}^{\dagger\mathrm{D}}$. The equations of motion are

$$\frac{d}{dt}\mathbf{x}=\mathbf{v}\ , \tag{9}$$

$$\frac{d}{dt}\mathbf{v}=-\omega_0^2\mathbf{x}-\frac{1}{m}\nabla_x V_{d,i}^{\mathbf{r}_0}(\mathbf{x})+\frac{e\eta}{m}\mathbf{E}_\perp(\mathbf{r}_0)\ , \tag{10}$$

$$\frac{d}{dt}a_{\mathbf{k},s}^{\mathrm{D}}=-iKa_{\mathbf{k},s}^{\mathrm{D}}-e\eta\frac{1}{\sqrt{\epsilon_0}}g(K)\mathbf{v}\cdot\mathcal{E}_{\mathbf{k},s}^{*\mathrm{D}}(\mathbf{r}_0)\ , \tag{11}$$

$$\frac{d}{dt}a_{\mathbf{k},s}^{\dagger\mathrm{D}}=iKa_{\mathbf{k},s}^{\dagger\mathrm{D}}-e\eta\frac{1}{\sqrt{\epsilon_0}}g(K)\mathbf{v}\cdot\mathcal{E}_{\mathbf{k},s}^{\mathrm{D}}(\mathbf{r}_0)\ , \tag{12}$$

$$\frac{d}{dt}a_{\mathbf{K},s}^{\mathrm{V}}=-iKa_{\mathbf{K},s}^{\mathrm{V}}-e\eta\frac{1}{\sqrt{\epsilon_0}}g(K)\mathbf{v}\cdot\mathcal{E}_{\mathbf{K},s}^{*\mathrm{V}}(\mathbf{r}_0)\ , \tag{13}$$

$$\frac{d}{dt}a_{\mathbf{K},s}^{\dagger\mathrm{V}}=iKa_{\mathbf{K},s}^{\dagger\mathrm{V}}-e\eta\frac{1}{\sqrt{\epsilon_0}}g(K)\mathbf{v}\cdot\mathcal{E}_{\mathbf{K},s}^{\mathrm{V}}(\mathbf{r}_0)\ , \tag{14}$$

where

$$\mathbf{E}_{\perp}(\mathbf{r}_0)=\frac{1}{(2\pi)^3\sqrt{\epsilon_0}}\sum_{s=1,2}\left\{\int_{k_3>0}d_3\mathbf{k}\,Kg(K)[a^{\mathrm{D}}_{\mathbf{k},s}\mathcal{E}^{\mathrm{D}}_{\mathbf{k},s}(\mathbf{r}_0)+a^{\dagger\mathrm{D}}_{\mathbf{k},s}\mathcal{E}^{*\mathrm{D}}_{\mathbf{k},s}(\mathbf{r}_0)]\right.$$
$$\left.+\int_{K_3<0}d_3\mathbf{K}\,Kg(K)[a^{\mathrm{V}}_{\mathbf{K},s}\mathcal{E}^{\mathrm{V}}_{\mathbf{K},s}(\mathbf{r}_0)+a^{\dagger\mathrm{V}}_{\mathbf{K},s}\mathcal{E}^{*\mathrm{V}}_{\mathbf{K},s}(\mathbf{r}_0)]\right\}. \tag{15}$$

These equations are valid either when the oscillator is placed in the vacuum ($\eta=1$), or in the dielectric ($\eta\neq1$). The most effective method to solve this set of equations is the Laplace transform method, $\tilde{f}(z)=\int_0^\infty e^{-zt}f(t)dt$. Solving Eqs. (11)–(14), e.g.,

$$\tilde{a}^{\mathrm{D}}_{\mathbf{k},s}(z)=\frac{1}{z+iK}\left[a^{\mathrm{D}}_{\mathbf{k},s}(0)-e\eta\frac{1}{\sqrt{\epsilon_0}}g(K)\tilde{\mathbf{v}}(z)\cdot\mathcal{E}^{*\mathrm{D}}_{\mathbf{k},s}(\mathbf{r}_0)\right], \tag{16}$$

one can eliminate the field variables from the equation of motion of the charge. Afterwards one gets

$$\mathbf{H}(z)\cdot\tilde{\mathbf{v}}(z)=\mathbf{F}(\mathbf{x}(0),\mathbf{v}(0),z)+\mathcal{A}_{\mathrm{field}}(0,z), \tag{17}$$

where the right hand side terms include the initial data for the oscillating electron (the first one) and the field (the second). To shorten the formulas we introduce the wave vectors $\mathbf{k}^{\mathrm{D}}=\mathbf{k}$ and $\mathbf{k}^{\mathrm{V}}=\mathbf{K}$,

$$\mathbf{F}(\mathbf{x}(0),\mathbf{v}(0),z)=(-\hat{\mathbf{D}}_e-\omega_0^2)\cdot\mathbf{x}(0)+z\mathbf{v}(0), \tag{18}$$

$$\mathcal{A}_{\mathrm{field}}(0,z)=\frac{e\eta z}{(2\pi)^3m\sqrt{\epsilon_0}}\sum_{s=1,2}\sum_{J=D,V}\int d^3\mathbf{k}^J Kg(K)\left[a^J_{\mathbf{k}^J,s}(0)\frac{\mathcal{E}^J_{\mathbf{k}^J,s}(\mathbf{r}_0)}{z+iK}+a^{\dagger J}_{\mathbf{k}^J,s}(0)\frac{\mathcal{E}^{*J}_{\mathbf{k}^J,s}(\mathbf{r}_0)}{z-iK}\right]. \tag{19}$$

The integration over $\mathbf{k}^{\mathrm{D}}$ extends to $k_3^{\mathrm{D}}>0$ only, while the integration over $\mathbf{k}^{\mathrm{V}}$ extends to $k_3^{\mathrm{V}}<0$. The resolvent matrix function is given by the following expression:

$$\mathbf{H}(z)=z^2+\omega_0^2+\hat{\mathbf{D}}_e+2z^2\frac{e^2\eta^2}{(2\pi)^3m\epsilon_0}\sum_{s=1,2}\sum_{J=\mathrm{V,D}}\int d_3\mathbf{k}^J Kg^2(K)\frac{\mathcal{E}^J_{\mathbf{k}^J,s}(\mathbf{r}_0)\mathcal{E}^{*J}_{\mathbf{k}^J,s}(\mathbf{r}_0)}{z^2+K^2}. \tag{20}$$

Important properties of the system dynamics, its damping and radiative frequency shifts, are described by this resolvent. For the selected modes of the electromagnetic (EM) field, $\mathcal{E}^{\mathrm{D}}_{\mathbf{k},s}(\mathbf{r})$ and $\mathcal{E}^{\mathrm{V}}_{\mathbf{K},s}(\mathbf{r})$, some structure of the coupling between the dipole and the field can be found. The picture is somehow different depending on whether the oscillator is placed in the vacuum or in the dielectric, so we will draw them separately. The resolvent function $\mathbf{H}(z)$ is expressed with the help of a three-dimensional integral over the wave vectors $\mathbf{k}$ or $\mathbf{K}$ parametrizing the field modes. The integration over only two variables: the cylindrical angle ϕ and the length of the wave vector, can be effectively performed. Thus the resolvent function can be expressed via a one-dimensional integral over the azimuthal angles Θ or θ.

A. Oscillator in vacuum

Introducing the explicit form of the field modes into the dyads $\mathcal{E}^J_{\mathbf{k}^J,s}(\mathbf{r}_0)\mathcal{E}^{*J}_{\mathbf{k}^J,s}(\mathbf{r}_0)$ we find terms that are independent of the position of the oscillator $\mathbf{r}_0$. For the oscillator placed in the vacuum these terms are the products of the incident components and the products of the reflected components of the V mode, Eqs. (A1) and (A2), and all the propagating D modes. All these terms combine together with the free oscillation part of $\mathbf{H}(z)$, $(z^2+\omega_0^2)$, to give the resolvent function of the oscillator interacting with the electromagnetic field in the free space, $H_0(z)$, which was calculated and discussed in [29]. Position dependent terms arise from the products of the incident-reflected parts of the V modes and the evanescent waves of the D modes. The product of the incident-reflected components takes the form of a standing wave and coupling to the $\mathcal{E}^{\mathrm{V}}_{\mathbf{K}}$ mode is proportional to $\cos(2Kh\cos\Theta)$. The coupling to $\mathcal{E}^{\mathrm{D}}_{\mathbf{k}}$ modes is proportional to the exponentially decreasing factor $\exp(-2Kh\sqrt{n^2\sin^2\theta-1})$. The complex independent variable z of the Laplace transform appears only in terms involving integrations over the length of $\mathbf{K}$ or $\mathbf{k}$. An expansion

$$\frac{K^2}{K^2+z^2}=1-z^2\frac{1}{K^2+z^2}$$

appears useful. All integrations involving the first term, i.e., "1," can be performed analytically. The corresponding term is denoted as $\hat{\mathbf{L}}$ in Eq. (21). The contributions of the second term can be integrated over the angle ϕ and the wave vector length K (or k) only. However, the K integration for the evanescent wave leads to special functions given in Appendix C. Finally, the resolvent function $\mathbf{H}(z)$ can be written in a form

$$\mathbf{H}=\hat{\mathbf{H}}_0+\hat{\mathbf{D}}_e+\hat{\mathbf{L}}+\hat{\mathbf{W}}+\hat{\mathbf{U}}, \tag{21}$$

where the free-space resolvent function

$$\hat{\mathbf{H}}_0(z)=\left[\omega_0^2+z^2\left[1+\frac{2}{3}\frac{e^2}{4\pi\epsilon_0 m}\frac{\Omega^2}{z+\Omega}\right]\right]\tilde{\mathbf{I}}, \tag{22}$$

where $\tilde{\mathbf{I}}$ is a unit matrix, the electrostatic part $\hat{\mathbf{D}}_e$ is given by Eq. (4), the evanescent D modes and a grazing angle of the V-mode contribution:

$$\hat{\mathbf{L}}=\frac{e^2}{4\pi\epsilon_0 m}z^2\frac{1}{4h}\frac{n^2-1}{(n^2+1)^2}\begin{bmatrix} n^2 & 0 & 0 \\ 0 & n^2 & 0 \\ 0 & 0 & 2(1+2n^2)\end{bmatrix}, \tag{23}$$

the V mode contribution:

$$\hat{\mathbf{W}}=-\frac{1}{2}\frac{e^2}{4\pi\epsilon_0 m}z^3\int_{\pi/2}^{\pi}d\Theta\sin\Theta e^{2hz\cos\Theta} \times\{R_{\mathrm{V},1}\hat{\mathbf{M}}_1+R_{\mathrm{V},2}\hat{\mathbf{M}}_2(\Theta)\}, \tag{24}$$

and the evanescent part of D modes:

$$\hat{\mathbf{U}}=-\frac{1}{2\pi}\frac{e^2z^3n^3}{4\pi\epsilon_0 m}\int_{\theta_c}^{\pi/2}d\theta(\sin\theta)F(2hz\sqrt{n^2\sin^2\theta-1}) \times\left\{\frac{1}{n^2}|T_{\mathrm{D},1}|^2\hat{\mathbf{M}}_1 +|T_{\mathrm{D},2}|^2\hat{\mathbf{M}}_3(\theta)\right\}. \tag{25}$$

The matrices appearing in the above equations, $\hat{\mathbf{M}}_1$, $\hat{\mathbf{M}}_2$, and $\hat{\mathbf{M}}_3$, result from the integration of the corresponding products of the polarization vectors over ϕ. Their explicit form is given in Appendix B. The function $F(az)$, expressed by special functions Si and Ci and defined in [39], is given in Appendix C. We point out that the cutoff function $g(K)$ appears only in the resolvent function $\hat{\mathbf{H}}_0$ of the free space. All the other terms do not require any tempering and we take $g(k)=K^{-1/2}$.

B. Oscillator in a dielectric

When the oscillator is placed in the dielectric, position independent terms originate from the V modes and the products of the incident-incident and reflected-reflected waves of the D modes (including propagating and evanescent waves). All these terms combine together with $z^2+\omega_0^2$ to the resolvent function of the oscillator interacting with the EM field in an infinitely extended dielectric medium:

$$\hat{\mathbf{H}}_0^{\mathrm{diel}}(z)=\left[\omega_0^2+z^2\left[1+\frac{2}{3}n\frac{e^2\eta^2}{4\pi\epsilon_0 m}\frac{\Omega_n^2}{z+\Omega_n}\right]\right]\hat{\mathbf{I}}. \tag{26}$$

This resolvent leads to a commonly accepted reduction of the excitation time due to emission of radiation in the dielectric, cf. [27],

$$\gamma_{\mathrm{diel}}=\frac{9n^5}{(2n^2+1)^2}\gamma_0. \tag{27}$$

The oscillator position dependent coupling terms come only from the product of the incident-reflected waves which form a standing-wave pattern. There are some differences between these contributions from the sector $\theta<\theta_C$ (propagating waves) and from the sector $\theta>\theta_C$ (evanescent waves). The $\mathcal{E}_{\mathbf{k},s}^{\mathrm{D}}$ mode contribution in the propagating sector is proportional to $\cos(2kh\cos\theta)$. The reflected waves in the evanescent sector gain some additional phase shift and the coupling is not only proportional to $\cos(2kh\cos\theta)$ but also terms proportional to $\sin(2kh\cos\theta)$ occur. The resolvent function $\mathbf{H}^{\mathrm{diel}}$ can be written in the following form:

$$\mathbf{H}^{\mathrm{diel}}=\hat{\mathbf{H}}_0^{\mathrm{diel}}\hat{\mathbf{D}}_e^{\mathrm{diel}}+\hat{\mathbf{L}}^{\mathrm{diel}}+\hat{\mathbf{W}}_p^{\mathrm{diel}}+\hat{\mathbf{W}}_{e1}^{\mathrm{diel}}+\hat{\mathbf{W}}_{e2}^{\mathrm{diel}}, \tag{28}$$

where the electrostatic part $\hat{\mathbf{D}}_e^{\mathrm{diel}}$ is given by Eq. (5) ($h<0$), and

$$\hat{\mathbf{L}}^{\mathrm{diel}}=\frac{e^2\eta^2}{4\pi\epsilon_0 m}z^2\frac{1}{4h}\frac{n^2-1}{(n^2+1)^2}\begin{bmatrix} 1 & 0 & 0 \\ 0 & 1 & 0 \\ 0 & 0 & 2(n^2+2)\end{bmatrix}. \tag{29}$$

The D-mode contribution in the propagating sector:

$$\hat{\mathbf{W}}_p^{\mathrm{diel}}=-\frac{1}{2}n\frac{e^2\eta^2}{4\pi\epsilon_0 m}z^3\int_0^{\theta_c}d\theta\sin\theta e^{2nhz\cos\theta} \times\{R_{\mathrm{D},1}\hat{\mathbf{M}}_1+R_{\mathrm{D},2}\hat{\mathbf{M}}_2(\theta)\}, \tag{30}$$

while the D-mode evanescent wave sector gives two contributions:

$$\hat{\mathbf{W}}_{e1}^{\mathrm{diel}}=-\frac{1}{2}n\frac{e^2\eta^2}{4\pi\epsilon_0 m}z^3\int_{\theta_C}^{\pi/2}d\theta\sin\theta e^{2nhz\cos\theta} \times\{\mathrm{Re}(R_{\mathrm{D},1})\hat{\mathbf{M}}_1 +\mathrm{Re}(R_{\mathrm{D},2})\hat{\mathbf{M}}_2(\theta)\} \tag{31}$$

and

$$\hat{\mathbf{W}}_{e2}^{\mathrm{diel}}=\frac{1}{2}n\frac{e^2\eta^2}{4\pi\epsilon_0 m}z^3\int_{\theta_c}^{\pi/2}d\theta(\sin\theta)G(-2nhz\cos\theta) \times\{\mathrm{Im}(R_{\mathrm{D},1})\hat{\mathbf{M}}_1 +\mathrm{Im}(R_{\mathrm{D},2})\hat{\mathbf{M}}_2(\theta)\}, \tag{32}$$

with the $G(s)$ function defined in Appendix C.

III. DECAY RATE AND FREQUENCY SHIFT

Time evolution of the system is given by functions obtained as inverse Laplace transformations ($\xi=0,1$):

$$\mathbf{f}^{\xi}(t)=\frac{1}{2\pi i}\int_{\Gamma}e^{zt}z^{\xi}\mathbf{H}^{-1}(z)dz, \tag{33}$$

where the contour Γ goes parallel to the imaginary axis from $-i\infty$ to $+i\infty$ and is shifted to the right of all singularities of the integrand functions.

To perform the inverse Laplace transformation one has to know the analytical properties of the inverse resolvent functions $\mathbf{H}^{-1}(z)$ or $\mathbf{H}^{\mathrm{diel}^{-1}}(z)$. As the resolvent matrices $\mathbf{H}$ are diagonal the matrix inversion is simple.

We can divide the oscillations of the dipole into two classes; oscillations parallel to the z axis (calling them "parallel") and oscillations perpendicular to the z axis (calling them "perpendicular"). Accordingly, we will denote the corresponding resolvent functions by $H_{\parallel}(z)$

and $H_{\perp}(z)$ and the time-resolvent functions by $f^{\xi}_{\parallel(\perp)}(t)$,

$$f^{\xi}_{\parallel(\perp)}(t)=\frac{1}{2\pi i}\int_{\Gamma}e^{zt}z^{\xi}H_{\parallel(\perp)}{}^{-1}(z)dz \ . \tag{34}$$

The resolvent functions $H(z)$ are multivalued because they include special functions: Si(z), Ci(z), Ei(z), and $E_1(z)$ which have a logarithmic branching point at $z=0$. To perform the inverse Laplace transformations we have to select proper Riemann surfaces and introduce cuts connecting the branching points at $z=0$ with the one at $z=\infty$. For all resolvent functions a convenient cut goes along the negative part of the real axis.

Properties of the functions $f^{\xi}_{\parallel(\perp)}(t)$ are determined by all poles of $H^{-1}_{\parallel(\perp)}(z)$ [the roots of $H_{\parallel(\perp)}(z)=0$] and integrals along the cut. The integrals along the cut contribute to, so called, nonexponential decay. In analogous problems of quantum optics all such nonexponential decays are extremely weak and out of any experimental observation.

Having in mind an analogy with a solution of two oscillator problem [30], one may expect that the equations $H_{\parallel}(z)=0$ and $H_{\perp}(z)=0$ have an infinite number of roots. All of them, except a pair of roots close to a free oscillation frequency, $z_0=\pm i\omega_0$, are unknown. It is generally believed and for the two oscillator problem shown [30], that the contribution of these unknown roots is small. They may be important in some fine transient evolution just after the initial moment. All observable effects depend on the roots that are close to $\pm i\omega_0$. Their accurate values can be determined using any iterative procedure that starts from $z_0=i\omega_0$, e.g., the Newton iteration:

$$z^{\alpha}_{n}=z^{\alpha}_{n-1}-\frac{H^{\alpha}(z^{\alpha}_{n-1})}{H^{\alpha\prime}(z^{\alpha}_{n-1})} \ . \tag{35}$$

The index α denotes either $\parallel$ or $\perp$ with additional specification if the oscillator is in the vacuum or in the dielectric. In Figs. 2 and 3 the radiative damping and the radiative frequency shift for "perpendicular" and "parallel" oscillations and for several refractive indices n, as a function of the dipole separation from the dielectric boundary, are shown. Because the EM coupling is very weak the iterative procedure can be limited to one iteration only. If we restrict accuracy to the terms of the order e^2 only, then $H^{\alpha\prime}(z^{\alpha}_{0})$ can be replaced by $\pm 2i\omega_0$ and we get explicit formulas for the oscillator excitation damping and its frequency shift.

$$\delta z^{\alpha}_{1}=i\delta\omega^{\alpha}-\gamma^{\alpha}=\frac{1}{2\omega_0}iH^{\alpha}(i\omega_0) \ . \tag{36}$$

Such formulas for the damping constant $\gamma_{\parallel}$ and $\gamma_{\perp}$ have already been obtained by Sommerfeld and repeated many times later. We wish to emphasize the role of the evanescent waves in the oscillator damping when the oscillator approaches the interface.

In the case of the interface with a perfect conductor, when the separation of the oscillator from the boundary goes to zero, $h\to 0$, the damping of "parallel" oscillations is enhanced by a factor of 2, while the damping of "perpendicular" oscillations vanishes. This contrasts with observed properties of radio wave propagation (Sommer-

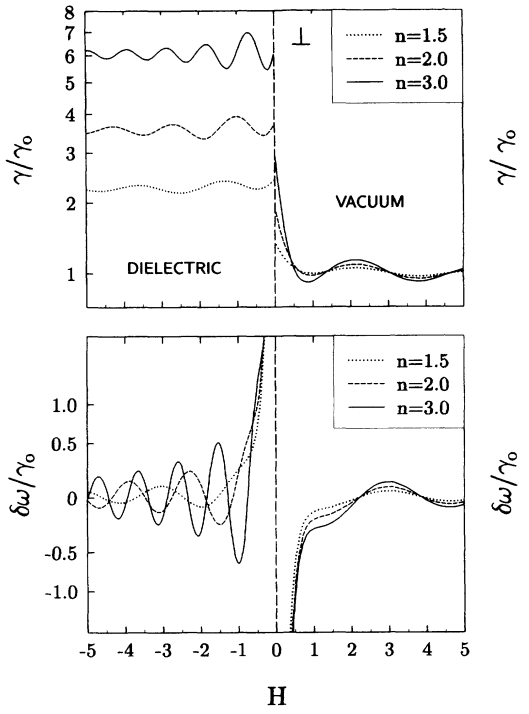

FIG. 2. Decay rate and frequency shift for perpendicular oscillations as a function of distance from the dielectric boundary ($H=\omega_0 h$).

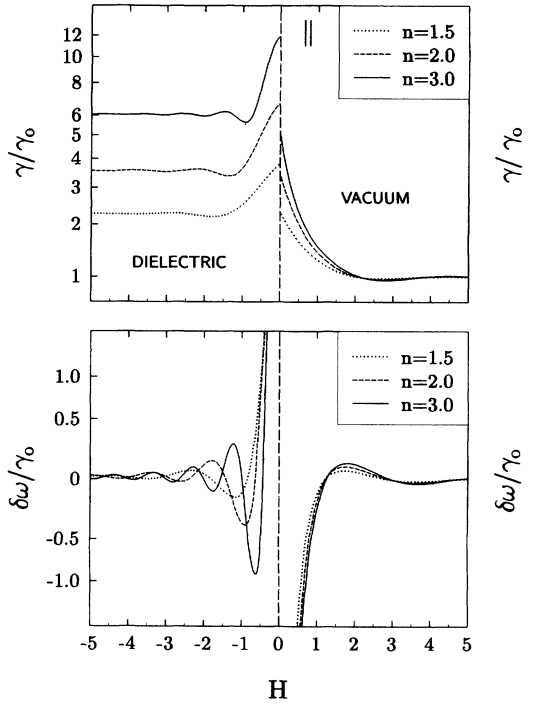

FIG. 3. Decay rate and frequency shift for parallel oscillations as a function of distance from the dielectric boundary.

feld) and atomic excitation damping in the Drexhage experiments. Both effects exhibit much stronger damping in this limit. Obviously, neither the earth surface nor the metallic substrate are perfect conductors and by taking into account their finite conductivity a good quantitative agreement with observations was reached. Those discussions claimed a dissipative nature of the media to be necessary for explanation of the observed damping enhancement. However, we point out that a critical factor in enhanced radiative damping, in the limit $h \to 0$, can come from the coupling of the oscillator to the evanescent modes. A similar conclusion, but reached in another way, was formulated in [25].

An analysis of the radiative frequency shifts presents more difficulties, and it is more difficult for an experimental observation. For larger distances from the dielectric boundary the frequency shifts show similar waving variations with distance as are shown by the radiative decays. However, in the limit $h \to 0$, the electrostatic shift becomes dominating. Then we get a divergent, van der Waals type frequency shift proportional to $|h|^{-3}$, "red" shift when the oscillator is in the vacuum, and a similar "blue" one when it is in the dielectric. As far as we know, only the first one has been recently confirmed in the experiment [15]. In addition to the above van der Waals frequency shift caused by coupling with the longitudinal field, one can distinguish oscillatory with the distance h shifts due to the coupling with the transverse fields and the shift $\propto h^{-1}$ caused by the evanescent waves and waves at the critical angle θ_c.

IV. RADIATION PATTERN

The angular characteristics of emission by an oscillating dipole located near the dielectric-vacuum interface were mostly discussed in the framework of classical electrodynamics. The Green function, first found by Sommerfeld, allows one to find the classical EM field corresponding to a given dipole current. Difficulties in application of the Green function are due to complex contour integral expressions representing the radiation field. During the long history of these problems quite good understanding of related phenomena has been reached. The evaluation methods have been developed and presented, e.g., in the monographs [3,4]. The Green function approach has been used to obtain the radiation pattern within the quantum-electrodynamical framework by Agarwal [17,18] and Arnoldus and George [23].

A typical radiation emission pattern of a dipole located near a dielectric boundary is shown in Figs. 4 and 5. When the dipole is far from the interface, $|h| \gg \lambda$, one can recognize, in the same half space in which the oscillator is placed, a number of lobes in the angular intensity characteristics. Classically, these radiation lobe patterns can be interpreted as an effect of the interference between the direct radiation waves emitted in a given direction and the waves which propagate in this half space after reflection from the interface. The number of lobes decreases when the dipole approaches the dielectric boundary. The lobe structure of the angular emission can be interpreted in terms of interference fringes appearing on a screen located near the radiation source. The configuration of our system resembles Lloyd's mirror.

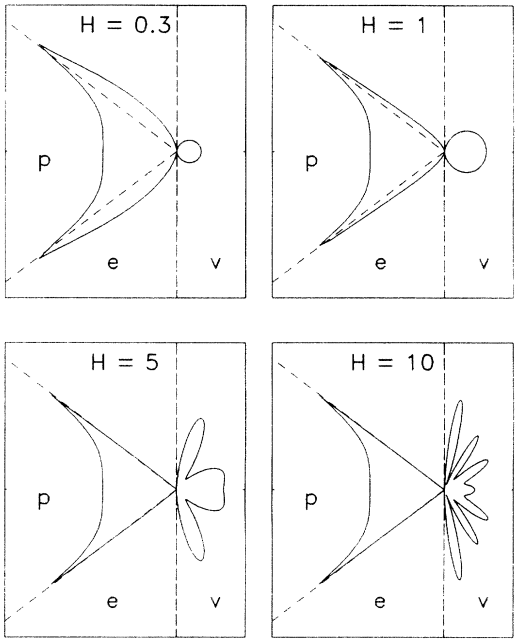

FIG. 4. Radiation pattern for an oscillator placed in the vacuum. The oscillator is excited in the **x** direction and the intensity of radiation of TE polarization, in the **x**-**z** plane, as a function of the angle θ, is shown. The dielectric refraction index $n = 1.5$.

When the oscillator approaches the interface from the vacuum side more and more radiation is emitted into the evanescent wave sector of the dielectric. In fact, for a selected polarization (TE) and the dipole orientation (per-

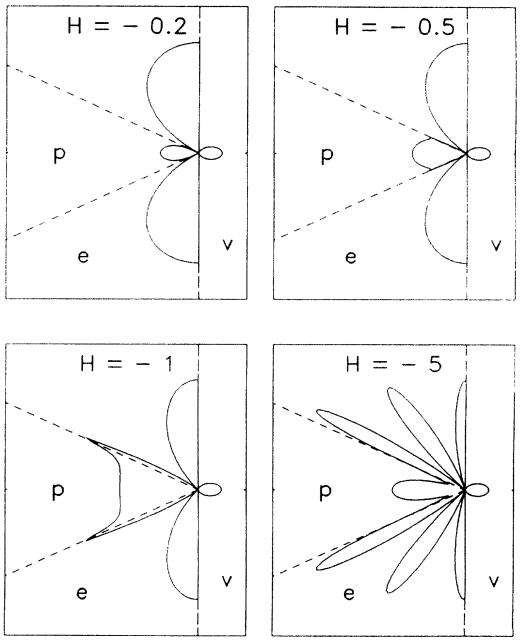

FIG. 5. The same for an oscillator in the dielectric.

pendicular), the maximum intensity is reached near the critical angle θ_C. This effect has been tested experimentally [31].

In this paper we want to present the quantum interpretation of the classical intensity directional pattern. We will use the most orthodox perturbation theory approach following the scheme given, e.g., in [37]. Within this approach the spontaneous radiation intensity is associated with the quantum transition probability, per unit time. During the transition the EM field state is changed from the vacuum state to a specified single photon state while at the same time the atom makes transition from the upper to lower energy state. While the perturbation procedure is clear and widely used in atomic physics for atoms radiating in vacuum, its application to problems of emission in space showing some structure, e.g., the problem discussed in this paper when the half space is filled with a dielectric, is unclear and has been rather avoided. Attempting to explain and clear up those difficulties we want to give the radiation intensity directional characteristics in terms of modes and photons that have been introduced by Carniglia and Mandel [34].

The Carniglia-Mandel modes are composed of triplet waves: incident, reflected, and transmitted ones. There is no obvious relation between an emission of the CM photons and the intensity of radiation in a given direction, measured by a photodetector placed at a given point and directed toward the source oscillator. When the oscillator and the detector are located in the vacuum half space one can expect that the counter is effected by the reflected "fragment" of V photons and the transmitted "fragment" of D photons.

A discussion of emission process in terms of the above photons has been given in [27]. Discussing a transition radiation, induced by an electron crossing the interface between two dielectrics, Glauber and Lewenstein assumed that the emitted photons of D and V type contribute incoherently to the detected field, so they postulated that the rate of detection is proportional to

$$dN \propto (P_{\mathrm{D}} T + P_{\mathrm{V}} R)\, d\Omega \ , \tag{37}$$

i.e., the sum of the probabilities of D- and V-photon emission, P_{D} and P_{V}, weighed by the transmission T and the reflection R coefficients.

However, the postulated equation seems to overlook a possibility of interference of photons of the two types, D and V [33]. When the detector measures the photon we cannot recognize, even in the gedanken experiment, whether the detection was due to absorption of the V photon or D photon. The fundamental lack of such distinction is the essence of the quantum interference effects [38]. Dealing with such quantum interference we have to sum the amplitudes, not the probabilities, for various paths connecting the initial and the final state. In our case, the final state of the photon detected within a given solid angle is connected to the initial vacuum photon state by the two indistinguishable paths corresponding to the emission of the D and V photons. Although different photons are independent (their creation and annihilation operators commute), their emission by one source cannot be viewed as an incoherent process. Such photon coherences are another aspect of the quantum interference phenomena.

The radiative transition between the initial and final states is caused by a coupling Hamiltonian

$$H_I = -\frac{e\eta}{m} \mathbf{p} \cdot \mathbf{A}(\mathbf{r}_0) \ . \tag{38}$$

The parameter η, as was explained earlier, allows modeling of local field effects when the oscillator is placed in the dielectric. In the model with a spherical vacuum microcavity surrounding the oscillator it is given by Eq. (7). When the oscillator is in the vacuum $\eta = 1$.

The initial state of the system corresponds to an excited oscillator state $|\psi_i\rangle$ (of energy E_i) and the vacuum photon state $|\Omega_{\mathrm{ph}}\rangle$. The final state corresponds to a deexcited oscillator $|\psi_f\rangle$ (of energy $E_f < E_i$) and a single photon state which we will specify in a moment.

The radiation spatial intensity pattern is not directly described by the Carniglia-Mandel photons due to, as discussed above, the lack of a unique correspondence between the angular distribution of the intensity and the photon types. The Carniglia-Mandel modes and the corresponding photons are parametrized by the incident wave vectors. It is more convenient to relate the directional intensity distribution to alternative outgoing CM photons which are parametrized by the final, outgoing, photon momenta, and not the incoming ones specified originally in [34]. These modes are described in more detail in Appendix A 2.

In the corresponding outgoing CM modes the outgoing wave is accompanied by two waves propagating toward the interface. One, moving in the same region as the outgoing wave, is an inverted reflected wave and can be called "pseudoreflected." The other one is moving in the complementary region, and it is an inverted transmitted wave, which may be called "pseudotransmitted." None of these "pseudoreflected" and "pseudotransmitted" waves can effect the photocounter as they are propagating out of the detector. Only the outgoing waves, which we use to parametrize the modes, may influence the detector. The detection of outgoing photons depends on the position of the photocounter. Its location in the vacuum makes it sensitive for the V-outgoing photon detection, while its location in the dielectric corresponds to the D-outgoing photon measurements.

The single V-outgoing-photon state parametrized by the wave vector K and the polarization s is described by

$$|(\mathbf{K},s)\rangle^{\mathrm{out}} = {}^{\mathrm{out}}a^{\dagger \mathrm{V}}_{\mathbf{K},s} |\Omega_{\mathrm{ph}}\rangle \ .$$

The probability of the emission per unit of time of this photon while the oscillator is changing its initial state $|\psi_i\rangle$ to the final state $|\psi_f\rangle$ according to a standard perturbation theory is

$$P^{\mathrm{V}}_{\mathbf{K},s} = 2\pi \frac{e^2\eta^2}{m^2} |\langle \psi_f|\mathbf{p}|\psi_i\rangle \cdot \langle \Omega_{\mathrm{ph}}|{}^{\mathrm{out}}a^{\mathrm{V}}_{\mathbf{K},s}\, \mathbf{A}(\mathbf{r}_0)|\Omega_{\mathrm{ph}}\rangle|^2 \times \delta(E_i - E_f - K) \ . \tag{39}$$

The field matrix element $\langle \Omega_{\mathrm{ph}}|{}^{\mathrm{out}}a^{\mathrm{V}}_{\mathbf{K},s}\, \mathbf{A}(\mathbf{r}_0)|\Omega_{\mathrm{ph}}\rangle$ can be easily calculated with the help of the expansion of the vector potential $\mathbf{A}$ given by Eq. (A20). One has

$$\langle \Omega_{\rm ph}|^{\rm out}a^{\rm V}_{\mathbf{K},s}\,\mathbf{A}(\mathbf{r}_0)|\Omega_{\rm ph}\rangle = \frac{i}{\sqrt{\epsilon_0 K}}\,{}^{\rm out}\mathcal{E}^{*\rm V}_{\mathbf{K},s}(\mathbf{r}_0)\ . \quad (40)$$

Thus the photon emission rate is

$$P^{\rm V}_{\mathbf{K},s} = \frac{2\pi}{\epsilon_0}e^2\eta^2 K\,|\mathbf{x}_{fi}\cdot{}^{\rm out}\mathcal{E}^{*\rm V}_{\mathbf{K},s}(\mathbf{r}_0)|^2\delta(E_{if}-K)\ , \quad (41)$$

where $\mathbf{x}_{fi}=\langle\psi_f|\mathbf{x}|\psi_i\rangle$ and $E_{if}=E_i-E_f$.

The outgoing modes ${}^{\rm out}\mathcal{E}^{*\rm V}_{\mathbf{K},\mathbf{s}}$ can be expressed in terms of the CM modes and the expansion is given in Appendix A. Inserting this expansion in Eq. (41) one can find a particular, coherent CM mode superposition which contributes to the radiation intensity in a direction of the wave vector $\mathbf{K}$ and polarization s. This procedure allows recovery of the missed interference term between the D photons and the V photons in the postulated Eq. (37). Thus we have (a superscript in indicates the original CM modes)

$$P^{\rm V}_{\mathbf{K},2} = \frac{2\pi}{\epsilon_0}e^2\eta^2 K\,|\mathbf{x}_{fi}\cdot[R_{\rm V,2}\,{}^{\rm in}\mathcal{E}^{*\rm V}_{\mathbf{K}^{\rm R},2}+T_{\rm V,2}\,{}^{\rm in}\mathcal{E}^{*\rm D}_{\mathbf{k},2}]|^2 \times\delta(E_{if}-K) \quad (42)$$

and

$$P^{\rm V}_{\mathbf{K},2} = {}^{\rm in}P^{\rm V}_{\mathbf{K}^{\rm R},2}R^2_{\rm V,2}+{}^{\rm in}P^{\rm D}_{\mathbf{k},2}T^2_{\rm V,2}+P_{\rm int}\ , \quad (43)$$

where an interference correction to Eq. (37) is

$$P_{\rm int} = \frac{2\pi}{\epsilon_0}e^2\eta^2 K R_{\rm V,2}T_{\rm V,2}\,2\,{\rm Re}[\mathbf{x}^*_{fi}\cdot{}^{\rm in}\mathcal{E}^{*\rm V}_{\mathbf{K}^{\rm R},2}\mathbf{x}_{fi}\cdot{}^{\rm in}\mathcal{E}^{\rm D}_{\mathbf{k},2}] \times\delta(E_{if}-K)\ . \quad (44)$$

Now, we will use again the outgoing modes in the discussion of the radiation emission. To get the intensity of radiation of the polarization s, emitted in the direction (Θ_0,ϕ_0), one must multiply $P^{\rm V}_{\mathbf{K},s}$ by the photon energy K, integrate over possible outgoing modes with the $\mathbf{K}$ vector pointing in this direction, and sum over possible final states $|\psi_f\rangle$ of the oscillator. Only states ~nserving energy may contribute to the radiation process.

$$\frac{dI^{\rm V}_{K,s}(\Theta_0,\phi_0)}{d\Omega} = \frac{1}{(2\pi)^3\sin\Theta_0}\times\sum_f\int_{K_3>0}d^3\mathbf{K}\,KP^{\rm V}_{\mathbf{K},s}\delta(\Theta-\Theta_0)\times\delta(\phi-\phi_0)\ . \quad (45)$$

Presence of $\delta(E_i-E_f-K)$ in $P^{\rm V}_{\mathbf{K},s}$ simplifies the integration and one gets $(0<\Theta_0<\pi/2)$

$$\frac{dI^{\rm V}_{K,s}(\Theta_0,\phi_0)}{d\Omega} = \frac{e^2\eta^2E^4_{if}}{4\pi^2\epsilon_0}\sum_f|\mathbf{x}_{fi}\cdot{}^{\rm out}\mathcal{E}^{*\rm V}_{\mathbf{K},s}(\mathbf{r}_0)|^2\ . \quad (46)$$

In an analogous way one can determine the intensity of radiation emitted into the dielectric. In this case one must look for a rate of emission of outgoing D photons associated with the outgoing D modes. The only new element requiring some attention is the integration over $\mathbf{k}$ while we still have $\delta(E_i-E_f-K)$. Thus one gets $(\pi>\theta_0>\pi/2)$

$$\frac{dI^{\rm D}_{K,s}(K,\theta_0,\phi_0)}{d\Omega} = \frac{e^2\eta^2E^4_{if}n^3}{4\pi^2\epsilon_0}\sum_f|\mathbf{x}_{fi}\cdot{}^{\rm out}\mathcal{E}^{*\rm D}_{\mathbf{k},\mathbf{s}}(\mathbf{r}_0)|^2\ . \quad (47)$$

The formulas (45) and (47) allow one to find the radiation intensity of two given polarizations, the same that have been chosen initially for the vector potential $\mathbf{A}$ expansion. We do not have to restrict ourselves to these two specified polarizations. We have the freedom to choose an arbitrary polarization according to the type of detector equipment and polarization filters selected. A general polarization state of the radiation in a given direction can be parametrized by two angles, α and δ. A corresponding single outgoing V-photon state is

$$|\mathbf{K}(\alpha,\delta)\rangle^{\rm out}=[(\cos\alpha)^{\rm out}a^{\dagger\rm V}_{\mathbf{K},1}+e^{i\delta}(\sin\alpha)^{\rm out}a^{\dagger\rm V}_{\mathbf{K},2}]|\Omega_{\rm ph}\rangle\ .$$

For $\delta=0$ we have a linear polarization with the polarization plane rotated along the $\mathbf{K}$ vector. The angles $\alpha=\pi/4$ and $\delta=\pm\pi/2$ lead to two circular polarizations. One can write analogous states for outgoing D photons. The intensity of radiation of the polarization (α,δ) for the outgoing V photons is

$$\frac{dI^{\rm V}_{K,\alpha,\delta}(\Theta_0,\phi_0)}{d\Omega} = \frac{e^2\eta^2E^4_{if}}{4\pi^2\epsilon_0}\sum_f|\mathbf{x}_{fi}\cdot[(\cos\alpha)^{\rm out}\mathcal{E}^{*\rm V}_{\mathbf{K},1}(\mathbf{r}_0)+e^{i\delta}(\sin\alpha)^{\rm out}\mathcal{E}^{*\rm V}_{\mathbf{K},2}(\mathbf{r}_0)]|^2 \quad (48)$$

and for the outgoing D photons

$$\frac{dI^{\rm D}_{K,\alpha,\delta}(\theta_0,\phi_0)}{d\Omega} = \frac{e^2\eta^2E^4_{if}n^3}{4\pi^2\epsilon_0}\sum_f|\mathbf{x}_{fi}\cdot[(\cos\alpha)^{\rm out}\mathcal{E}^{*\rm D}_{\mathbf{k},1}(\mathbf{r}_0)+e^{i\delta}(\sin\alpha)^{\rm out}\mathcal{E}^{*D}_{\mathbf{k},2}(\mathbf{r}_0)]|^2\ . \quad (49)$$

The total intensity of radiation without any polarization specification is given by the sum of the intensities for any two orthogonal polarizations $(J=\rm V,D)$

$$\frac{dI^J_K}{d\Omega} = \frac{dI^J_{K,1}}{d\Omega}+\frac{dI^J_{K,2}}{d\Omega} = \frac{dI^J_{K,\alpha,\delta}}{d\Omega}+\frac{dI^J_{K,\alpha+\pi/2,\delta}}{d\Omega} = \frac{dI^J_{K,\alpha,\delta}}{d\Omega}+\frac{dI^J_{K,\alpha,\delta+\pi}}{d\Omega}\ . \quad (50)$$

Using the explicit form of the mode functions, Eqs. (A1)–(A4), and assuming that the oscillator is in the vacuum we get for the intensity of radiation of the polarization $s=1$ in the vacuum half space

$$\frac{dI^{\rm V}_{K,1}(\Theta_0,\phi_0)}{d\Omega} = \frac{e^2E^4_{if}}{8\pi^2\epsilon_0}\sum_f|\mathbf{x}_{fi}\cdot\mathbf{e}|^2\{1+R^2_{\rm V,1}+2R_{\rm V,1}\cos(2Kh\cos\Theta_0)\}\ . \quad (51)$$

The corresponding intensity distribution for the second polarization, $s=2$, has a similar structure although its geometrical form is more complicated,

$$\frac{dI^{\mathrm{V}}_{K,2}(\Theta_0,\phi_0)}{d\Omega}=\frac{e^2E_{if}^4}{8\pi^2\epsilon_0}\sum_f \mathcal{T}_{fi}+\mathcal{C}_{fi}\cos(2Kh\cos\Theta_0)+\mathcal{S}_{fi}\sin(2Kh\cos\Theta_0)\ , \tag{52}$$

where ($\mathbf{c}=\mathbf{c}_\parallel+\mathbf{c}_\perp$, with respect to the direction of the z axis)

$$\mathcal{T}_{fi}=(1+R_{v,2}^2)[|\mathbf{x}_{fi}\cdot(\mathbf{c}_\perp\times\mathbf{e})|^2+|\mathbf{x}_{fi}\cdot(\mathbf{c}_\parallel\times\mathbf{e})|^2]+2(1-R_{\mathrm{V},2}^2)\,\mathrm{Re}[(\mathbf{x}_{fi}\cdot\mathbf{c}_\perp\times\mathbf{e})(\mathbf{x}_{fi}^*\cdot\mathbf{c}_\parallel\times\mathbf{e})]\ ,$$

$$\mathcal{C}_{fi}=2R_{\mathrm{V},2}[|\mathbf{x}_{fi}\cdot(\mathbf{c}_\perp\times\mathbf{e})|^2-|\mathbf{x}_{fi}\cdot(\mathbf{c}_\parallel\times\mathbf{e})|^2]\ ,$$

$$\mathcal{S}_{fi}=-4R_{\mathrm{V},2}\,\mathrm{Im}[(\mathbf{x}_{fi}\cdot\mathbf{c}_\perp\times\mathbf{e})(\mathbf{x}_{fi}^*\cdot\mathbf{c}_\parallel\times\mathbf{e})]\ .$$

These equations allow one to give a new interpretation of the origin of the lobe structure of the radiation intensity characteristics. The modes contributing to the emission of radiation in the same half space in which the oscillator is placed are coupled with the oscillator via a superposition of the outgoing and "pseudo" reflected waves. For each mode these waves form a partially standing-wave pattern. This combination of waves shows a natural intensity modulation when a separation from the interface is changed. The "strength" of the coupling is proportional to the amplitude of a given mode at the oscillator position. So, the intensity of radiation in a particular direction may vanish if the corresponding out mode has a node at this position. For other modes this position may coincide with the antinode of the mode and then the radiation intensity in a corresponding direction reaches its maximum. The lobe pattern is prominent if standing-wave structures are well developed and the oscillator is positioned at a perfect node for some modes and at perfect antinodes for other nodes. Such conditions are fulfilled when the oscillator separation from the interface is of the order of a few wavelengths, $h\geq N\lambda$, and radiation is observed at small angles measured from the interface, i.e., $0<\pi/2-\Theta_0\ll 1$.

In the half space occupied by the dielectric one must distinguish the propagation wave sector ($\pi-\theta_C<\theta<\pi$) and the evanescent wave sector ($\pi/2<\theta<\pi-\theta_C$). One gets, in the propagation wave sector,

$$\frac{dI^{\mathrm{D}}_{K,1}(\theta_0,\phi_0)}{d\Omega}=\frac{ne^2E_{if}^4}{8\pi^2\epsilon_0}\sum_f|\mathbf{x}_{fi}\cdot\mathbf{e}|^2T_{\mathrm{D},1}^2\ , \tag{53}$$

$$\frac{dI^{\mathrm{D}}_{K,2}(\theta_0,\phi_0)}{d\Omega}=\frac{n^3e^2E_{if}^4}{8\pi^2\epsilon_0}\sum_f|\mathbf{x}_{fi}\cdot\mathbf{c}\times\mathbf{e}|^2T_{\mathrm{D},2}^2\ , \tag{54}$$

and in the evanescent wave sector,

$$\frac{dI^{\mathrm{D}}_{K,1}(\theta_0,\phi_0)}{d\Omega}=\frac{ne^2E_{if}^4}{8\pi^2\epsilon_0}\sum_f|\mathbf{x}_{fi}\cdot\mathbf{e}|^2|T_{\mathrm{D},1}|^2\times e^{-2Kh\sqrt{n^2\sin^2\theta_0-1}}\ , \tag{55}$$

$$\frac{dI^{\mathrm{D}}_{K,2}(\theta_0,\phi_0)}{d\Omega}=\frac{n^3e^2E_{if}^4}{8\pi^2\epsilon_0}\sum_f|\mathbf{x}_{fi}\cdot\mathbf{c}\times\mathbf{e}|^2|T_{\mathrm{D},2}|^2\times e^{-2Kh\sqrt{n^2\sin^2\theta_0-1}}\ . \tag{56}$$

The lobe structure of the radiation intensity distribution cannot occur in this half space. In this half space coupling of the modes to the oscillator is given by the "pseudo" transmitted waves. For these waves a characteristic standing-wave pattern is not present. As a result, the radiation emitted into the dielectric in the propagation wave sector does not show any angular intensity dependence on the oscillator position. However, there is such dependence for emission into the evanescent wave sector. The radiation intensity decreases exponentially with respect to the distance if the oscillator is moved away from the interface.

Now, we consider a radiation pattern when the oscillator is located in the dielectric. The radiation intensity in the vacuum half space is

$$\frac{dI^{\mathrm{V}}_{K,1}(\Theta_0,\phi_0)}{d\Omega}=\frac{e^2\eta^2E_{if}^4}{8\pi^2\epsilon_0}\sum_f|\mathbf{x}_{fi}\cdot\mathbf{e}|^2T_{\mathrm{V},1}^2\ , \tag{57}$$

$$\frac{dI^{\mathrm{V}}_{K,2}(\Theta_0,\phi_0)}{d\Omega}=\frac{e^2\eta^2E_{if}^4}{8\pi^2\epsilon_0n^2}\sum_f|\mathbf{x}_{fi}\cdot\hat{\mathbf{k}}\times\mathbf{e}|^2T_{\mathrm{V},2}^2\ . \tag{58}$$

In the second equation $\hat{\mathbf{k}}$ must be expressed in terms of the angles Θ_0,ϕ, i.e.,

$$\hat{\mathbf{k}}=1/n(\sin\Theta_0\cos\phi,\sin\Theta_0\sin\phi,\sqrt{n^2-\sin^2\Theta_0})\ .$$

In the dielectric half space one gets

$$\frac{dI^{\mathrm{D}}_{K,1}(\theta_0,\phi_0)}{d\Omega}=\frac{e^2n\eta^2E_{if}^4}{8\pi^2\epsilon_0}\sum_f|\mathbf{x}_{fi}\cdot\mathbf{e}|^2\times\{1+|R_{\mathrm{D},1}|^2+2\,\mathrm{Re}[R_{\mathrm{D},1}e^{-2ik_3h}]\}\ , \tag{59}$$

$$\frac{dI^{\mathrm{D}}_{K,2}(\theta_0,\phi_0)}{d\Omega}=\frac{e^2n\eta^2E_{if}^4}{8\pi^2\epsilon_0}\sum_f\mathcal{D}_{fi}+\mathcal{H}_{fi}+\mathcal{L}_{fi}\ , \tag{60}$$

where ($\hat{\mathbf{k}}=\boldsymbol{\kappa}_\parallel+\boldsymbol{\kappa}_\perp$)

$$\mathcal{D}_{fi}=(1+|R_{\mathrm{D},2}|^2)[|\mathbf{x}_{fi}\cdot(\boldsymbol{\kappa}_\perp\times\mathbf{e})|^2+|\mathbf{x}_{fi}\cdot(\boldsymbol{\kappa}_\parallel\times\mathbf{e})|^2]+2(1-|R_{\mathrm{D},2}|^2)\mathrm{Re}[(\mathbf{x}_{fi}\cdot\boldsymbol{\kappa}_\perp\times\mathbf{e})(\mathbf{x}_{fi}^*\cdot\boldsymbol{\kappa}_\parallel\times\mathbf{e})]\ ,$$

$$\mathcal{H}_{fi}=2\mathrm{Re}[R_{\mathrm{D},2}e^{-2ik_3h}][|\mathbf{x}_{fi}\cdot(\boldsymbol{\kappa}_\perp\times\mathbf{e})|^2-|\mathbf{x}_{fi}\cdot(\boldsymbol{\kappa}_\parallel\times\mathbf{e})|^2]\ ,$$

$$\mathcal{L}_{fi}=-4\,\mathrm{Im}[R_{\mathrm{D},2}^*e^{2ik_3h}]\mathrm{Im}[(\mathbf{x}_{fi}\cdot\boldsymbol{\kappa}_\perp\times\mathbf{e})(\mathbf{x}_{fi}^*\cdot\boldsymbol{\kappa}_\parallel\times\mathbf{e})]\ .$$

The radiation patterns for several characteristic dipole positions are shown in Figs. 4 (for the dipole in the vacuum) and 5 (for one in the dielectric). We point out that when the oscillator approaches the interface from the vacuum side the lobes are vanishing, the total radiation into the vacuum half space is decreasing, while the radiation into the evanescent sector of the dielectric is increasing. The increase of emission into the evanescent sector

compensates the decrease of emission into the vacuum sector, so the total excitation decay constant is increasing as was derived in the preceding section and shown in Figs. 3 and 4. Our illustrations are given for a dielectric of a refraction index $n=1.5$. Even for such a moderate refraction index a dominant part of the emitted radiation for the oscillator close to the interface goes into the dielectric. This property would be more striking for dielectrics with larger refraction index n.

V. FINAL REMARKS

We have studied the coupling of a harmonic oscillator, located near a plane dielectric-vacuum interface, with electromagnetic radiation. The usefulness of the field modes which, in a given space structure, solve the free field Maxwell equations together with appropriate boundary conditions, has been shown. These free field modes define also photons which in a natural way emerge in a given environment configuration. Our discussion has concerned the simplest possible structured space, i.e., a lossless and nondispersive dielectric with a planar interface, for which case the natural modes, described by Carniglia and Mandel, were composed of triple waves connected according to the Fresnel formulas. Our approach and treatment can be extended to more general systems, more general configurations that can be more relevant to specific cavity quantum electrodynamics experiments. As we have already mentioned in the Introduction, the harmonic oscillator model can be directly applied to nonrelativistic electrons orbiting in a uniform static magnetic field.

Many results of this paper concerning radiative decay time and radiation intensity pattern are equivalent to the classical ones and had been obtained by Sommerfeld and others who generalized his approach. However, there are some conceptual differences between our and Sommerfeld types of approach. The Sommerfeld treatment was based on a solution of radiation by a dipole antenna driven by a given current. Therefore his antenna was a nonautonomous system. On the contrary, in our approach the oscillating dipole and the electromagnetic field form mutually coupled subsystems of a single autonomous system. Our approach allows us to solve the initial data problem for the total system. The spontaneous emission is due to the initial excitation of the dipole. All properties of the emitted light are results of the evolution of the total system.

ACKNOWLEDGMENTS

The authors would like to thank A. Błędowski, J. J. Fisz, M. Gajda, J. Mostowski, A. Raczyński, K. Rzążewski, and J. Zaremba for many stimulating discussions as well as B. G. Wybourne for critical reading of the manuscript. This work has been supported by Grant No. 2 P302 009 04 from the State Committee for Scientific Research.

APPENDIX A

1. Carniglia-Mandel modes

In this appendix we rewrite the Carniglia-Mandel modes of the electromagnetic field when the left half space ($z<0$) is filled with an ideal nonmagnetic, transparent, homogeneous, isotropic dielectric of the refractive index n (see Fig. 6). The half-space $z>0$ is empty.

Plane waves incident on the interface will be accompanied by reflected and transmitted waves. It is convenient to distinguish two classes of modes, or two polarizations, transverse electric (TE) modes and transverse magnetic (TM) ones. For the TE (TM) modes the electric (magnetic) field is transverse to the z axis, i.e., tangential to the interface. In addition to the classification according to the wave polarization one can further classify the modes depending on whether the incident wave is coming to the interface from the dielectric side or from the vacuum side. One can name the corresponding modes the D modes and the V modes.

Each mode is characterized by its frequency ω. We denote its wave vectors in the dielectric by a lower-case letter ($\mathbf{k}$) and in the vacuum by an upper-case one ($\mathbf{K}$). The frequency ω is given by $\omega=|\mathbf{K}|=|\mathbf{k}|/n=K=k/n$. The tangential component of the wave vectors $\mathbf{k}$ and $\mathbf{K}$ continues across the dielectric-vacuum interface, $\mathbf{k}_{\tan}=\mathbf{K}_{\tan}$, while the third components of the wave vectors, $k_3=\pm\sqrt{k^2-|\mathbf{k}_{\tan}|^2}$ and $K_3=\pm\sqrt{K^2-|\mathbf{K}_{\tan}|^2}$, are discontinuous. In the dielectric the wave vector $\mathbf{k}$ is always real. The corresponding wave vector in the vacuum, $\mathbf{K}$, may be complex, when $|\mathbf{K}_{\tan}|^2>K^2$. The modes for which the wave vector $\mathbf{K}$ is complex are called evanescent. The others are called propagation modes.

An angle between the z axis and the wave vector in the dielectric is denoted by θ and the corresponding angle in the vacuum by Θ. For the propagation modes the continuity of the tangential components of $\mathbf{k}$ and $\mathbf{K}$ gives the Snell law $n\sin\theta=\sin\Theta$ and one has

$$k_3=k\cos\theta=\mathrm{sgn}(\pi/2-\Theta)K\sqrt{n^2-\sin^2\Theta}\ ,$$

$$K_3=K\cos\Theta=\mathrm{sgn}(\pi/2-\theta)K\sqrt{1-n^2\sin^2\theta},\quad n\sin\theta<1\ .$$

For the evanescent waves one can specify only the direction of propagation in the dielectric θ (Θ is complex). For these waves one has

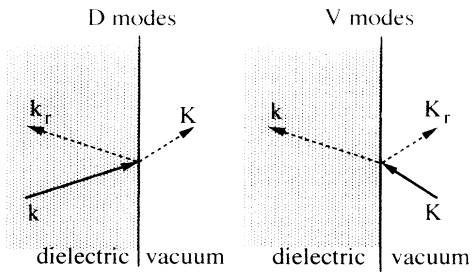

FIG. 6. Carniglia-Mandel dielectric-vacuum modes.

$$K_3 = i|\mathbf{K}|\sqrt{n^2\sin^2\theta - 1}\ .$$

One can point out that for the D modes k_3 (and K_3 for the propagation modes) are positive, implying

$$0<\Theta<\pi/2,\quad 0<\theta<\pi/2\ ,$$

while for the V modes the third components K_3 and k_3 are negative, implying

$$\pi/2<\Theta<\pi,\quad \pi-\theta_c<\theta<\pi\ .$$

Only the D modes may exist as the evanescent waves. For them

$$\pi/2>\theta>\theta_C=\arcsin 1/n\ .$$

The CM modes are specified as follows. The polarization index s is $s=1$ for the TE and $s=2$ for the TM polarizations. The V modes are specified by the incident wave vector in the vacuum $\mathbf{K}$, while the D modes are specified by the incident vector in the dielectric $\mathbf{k}$. We get for the V modes

$$\mathcal{E}^{\mathrm{V}}_{\mathbf{K},1}(\mathbf{r}) = \begin{cases} \frac{1}{\sqrt{2}}\hat{\mathbf{e}}T_{\mathrm{V},1}e^{i\mathbf{k}\cdot\mathbf{r}}, & z<0 \\ \frac{1}{\sqrt{2}}\hat{\mathbf{e}}(e^{i\mathbf{K}\cdot\mathbf{r}}+R_{\mathrm{V},1}e^{i\mathbf{K}^R\cdot\mathbf{r}}), & z>0 \end{cases} \tag{A1}$$

$$\mathcal{E}^{\mathrm{V}}_{\mathbf{K},2}(\mathbf{r}) = \begin{cases} -\frac{1}{\sqrt{2n}}\hat{\mathbf{k}}\times\hat{\mathbf{e}}T_{\mathrm{V},2}e^{i\mathbf{k}\cdot\mathbf{r}}, & z<0 \\ -\frac{1}{\sqrt{2}}(\hat{\mathbf{c}}\times\hat{\mathbf{e}}e^{i\mathbf{K}\cdot\mathbf{r}}+R_{\mathrm{V},2}\hat{\mathbf{c}}^R\times\hat{\mathbf{e}}e^{i\mathbf{K}^R\cdot\mathbf{r}}), & z>0\ . \end{cases} \tag{A2}$$

The D modes are given by

$$\mathcal{E}^{\mathrm{D}}_{\mathbf{k},1}(\mathbf{r}) = \begin{cases} \frac{1}{\sqrt{2'n}}\hat{\mathbf{e}}(e^{i\mathbf{k}\cdot\mathbf{r}}+R_{\mathrm{D},1}e^{i\mathbf{k}^R\cdot\mathbf{r}}), & z<0 \\ \frac{1}{\sqrt{2'n}}\hat{\mathbf{e}}T_{\mathrm{D},1}e^{i\mathbf{K}\cdot\mathbf{r}}, & z>0 \end{cases} \tag{A3}$$

$$\mathcal{E}^{\mathrm{D}}_{\mathbf{k},2}(\mathbf{r}) = \begin{cases} -\frac{1}{\sqrt{2'n}}(\hat{\mathbf{k}}\times\hat{\mathbf{e}}e^{i\mathbf{k}\cdot\mathbf{r}}+R_{\mathrm{D},2}\hat{\mathbf{k}}^R\times\hat{\mathbf{e}}e^{i\mathbf{k}^R\cdot\mathbf{r}}), & z<0 \\ -\frac{1}{\sqrt{2}}\hat{\mathbf{c}}\times\hat{\mathbf{e}}T_{\mathrm{D},2}e^{i\mathbf{K}\cdot\mathbf{r}}, & z>0\ . \end{cases} \tag{A4}$$

In these equations $\hat{\mathbf{e}}$ are the unit vectors in the x-y plane and perpendicular to the $\mathbf{k},\mathbf{K}$ wave vectors. They are polarization vectors for the TE modes. The vectors $\hat{\mathbf{k}}$ and $\hat{\mathbf{c}}$ are the unit vectors in the direction $\mathbf{k}$ and $\mathbf{K}$, respectively. Notice that $\hat{\mathbf{c}}$ can be complex for the evanescent waves. The reflected wave vectors are

$$\mathbf{k}^R=(k_1,k_2,-k_3)\quad\text{and}\quad\mathbf{K}^R=(K_1,K_2,-K_3)\ .$$

The Fresnel reflection and transmission coefficients are given by

$$\begin{aligned} R_{\mathrm{V},1} &= \frac{K_3-k_3}{K_3+k_3}\ , \\ T_{\mathrm{V},1} &= \frac{2K_3}{K_3+k_3}\ , \\ R_{\mathrm{V},2} &= \frac{n^2K_3-k_3}{n^2K_3+k_3}\ , \\ T_{\mathrm{V},2} &= \frac{2n^2K_3}{n^2K_3+k_3}\ , \\ R_{\mathrm{D},1} &= \frac{k_3-K_3}{K_3+k_3}\ , \\ T_{\mathrm{D},1} &= \frac{2k_3}{K_3+k_3}\ , \\ R_{\mathrm{D},2} &= \frac{k_3-n^2K_3}{k_3+n^2K_3}\ , \\ T_{\mathrm{D},2} &= \frac{2k_3}{k_3+n^2K_3}\ . \end{aligned} \tag{A5}$$

The Fresnel coefficients depend only on the direction of propagation and can be expressed either by the propagation angle in the dielectric θ, or the one in the vacuum Θ, whatever is convenient. They are real for all propagating modes and complex for the evanescent D modes. For those evanescent modes we take $K_3=i|K_3|$, so $|R_{\mathrm{D},1}|=|R_{\mathrm{D},2}|=1$.

The CM modes written above form an orthogonal complete set. They are normalized according to

$$\int d_3r n^2(z)\mathcal{E}^{*\mathrm{V}}_{\mathbf{K},s}(\mathbf{r})\cdot\mathcal{E}^{\mathrm{V}}_{\mathbf{K}',s'}(\mathbf{r}) = \tfrac{1}{2}(2\pi)^3\delta_{s,s'}\delta_3(\mathbf{K}-\mathbf{K}')\ , \tag{A6}$$

$$\int d_3r n^2(z)\mathcal{E}^{*\mathrm{D}}_{\mathbf{k},s}(\mathbf{r})\cdot\mathcal{E}^{\mathrm{D}}_{\mathbf{k}',s'}(\mathbf{r}) = \tfrac{1}{2}(2\pi)^3\delta_{s,s'}\delta_3(\mathbf{k}-\mathbf{k}')\ . \tag{A7}$$

The modes can be used to express quantum EM field operators. One can introduce the annihilation and creation operators $a^{\mathrm{V}}_{\mathbf{K},s}, a^{\dagger\mathrm{V}}_{\mathbf{K},s}, a^{\mathrm{D}}_{\mathbf{k},s}, a^{\dagger\mathrm{D}}_{\mathbf{k},s}$ and postulate standard canonical commutation relations:

$$[a^{\mathrm{V}}_{\mathbf{K},s}, a^{\dagger\mathrm{V}}_{\mathbf{P},u}] = (2\pi)^3\delta_{s,u}\delta_3(\mathbf{P}-\mathbf{K})\ ,$$

$$[a^{\mathrm{D}}_{\mathbf{k},s}, a^{\dagger\mathrm{D}}_{\mathbf{p},u}] = (2\pi)^3\delta_{s,u}\delta_3(\mathbf{p}-\mathbf{k})\ .$$

The creation and annihilation operators can be associated with creation and annihilation of photons in states given by the corresponding modes.

The operator of the vector potential of the EM field can be represented as

$$\mathbf{A}(\mathbf{r}) = \frac{-i}{(2\pi)^3\sqrt{\epsilon_0}}\sum_{s=1,2}\left\{\int_{k_3>0}d_3\mathbf{k}\frac{1}{\sqrt{K}}[a^{\mathrm{D}}_{\mathbf{k},s}\mathcal{E}^{\mathrm{D}}_{\mathbf{k},s} - a^{\dagger\mathrm{D}}_{\mathbf{k},s}\mathcal{E}^{*\mathrm{D}}_{\mathbf{k},s}] + \int_{K_3<0}d_3\mathbf{K}\frac{1}{\sqrt{K}}[a^{\mathrm{V}}_{\mathbf{K},s}\mathcal{E}^{\mathrm{V}}_{\mathbf{K},s} - a^{\dagger\mathrm{V}}_{\mathbf{K},s}\mathcal{E}^{*\mathrm{V}}_{\mathbf{K},s}]\right\}\ . \tag{A8}$$

2. Outgoing modes

The CM modes introduced and described above are parametrized by the wave vector of the incident waves. One can introduce an equivalent set of modes which are parametrized by the outgoing waves and outgoing wave vectors (see Fig. 7). The other set of modes is more convenient in discussions of the radiation emission problems. These outgoing modes

$$^{\text{out}}\mathcal{E}^{\text{V}}_{\mathbf{K},s}(\mathbf{r}) \quad \text{and} \quad ^{\text{out}}\mathcal{E}^{\text{D}}_{\mathbf{k},s}(\mathbf{r})$$

are given by the same structural expressions as $\mathcal{E}^{\text{V}}_{\mathbf{K},s}(\mathbf{r})$ and $\mathcal{E}^{\text{D}}_{\mathbf{k},s}(\mathbf{r})$, except that now the outgoing V modes have $K_3>0$ while for outgoing D modes $k_3<0$. This is also true for the outgoing D modes in the evanescent sector. For all the outgoing D modes we should simply take consequently $\pi/2<\theta<\pi$ in expressions (A3) and (A4). When $\pi-\theta_C<\theta<\pi$ we get automatically a correct form of the evanescent outgoing D modes. The outgoing modes also form a complete orthonormal set of modes. They can be expressed in terms of the incoming modes (the ordinary CM modes), and vice versa. For the propagating modes

$$^{\text{out}}\mathcal{E}^{\text{V}}_{\mathbf{K},1}=R_{\text{V},1}\mathcal{E}^{\text{V}}_{\mathbf{K}^R,1}+nT_{\text{V},1}\mathcal{E}^{\text{D}}_{\mathbf{k},1}\ , \tag{A9}$$

$$^{\text{out}}\mathcal{E}^{\text{D}}_{\mathbf{k},1}=\frac{1}{n}T_{\text{D},1}\mathcal{E}^{\text{V}}_{\mathbf{K},1}+R_{\text{D},1}\mathcal{E}^{\text{D}}_{\mathbf{k}^R,1}\ , \tag{A10}$$

and

$$^{\text{out}}\mathcal{E}^{\text{V}}_{\mathbf{K},2}=R_{\text{V},2}\mathcal{E}^{\text{V}}_{\mathbf{K}^R,2}+T_{\text{V},2}\mathcal{E}^{\text{D}}_{\mathbf{k},2}\ , \tag{A11}$$

$$^{\text{out}}\mathcal{E}^{\text{D}}_{\mathbf{k},2}=T_{\text{D},2}\mathcal{E}^{\text{V}}_{\mathbf{K},2}+R_{\text{D},2}\mathcal{E}^{\text{D}}_{\mathbf{k}^R,2}\ . \tag{A12}$$

For the evanescent modes these equations simplify, as there are no evanescent V modes. In this case $^{\text{out}}\mathcal{E}^{\text{D}}_{\mathbf{k},s}$ and $\mathcal{E}^{\text{D}}_{\mathbf{k}^R,s}$ are simply proportional, and

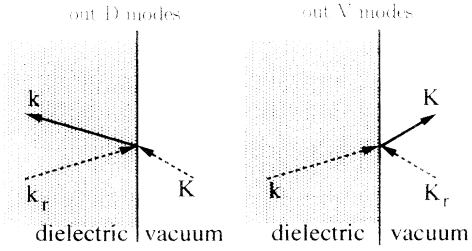

FIG. 7. Outgoing dielectric-vacuum modes.

$$^{\text{out}}\mathcal{E}^{\text{D}}_{\mathbf{k},s}=R^{*}_{\text{D},s}(\theta^R)\mathcal{E}^{\text{D}}_{\mathbf{k}^R,s}\ . \tag{A13}$$

Similar relations can be given for the "out" annihilation and creation operators $^{\text{out}}a^{\text{V}}_{\mathbf{K},s}$, $^{\text{out}}a^{\dagger\text{V}}_{\mathbf{K},s}$, $^{\text{out}}a^{\text{D}}_{\mathbf{k},s}$, $^{\text{out}}a^{\dagger\text{D}}_{\mathbf{k},s}$. In the propagating sector we have

$$^{\text{out}}a^{\text{V}}_{\mathbf{K},1}=R_{\text{V},1}a^{\text{V}}_{\mathbf{K}^R,1}+nT_{\text{V},1}a^{\text{D}}_{\mathbf{k},1}\ , \tag{A14}$$

$$^{\text{out}}a^{\text{D}}_{\mathbf{k},1}=\frac{1}{n}T_{\text{D},1}a^{\text{V}}_{\mathbf{K},1}+R_{\text{D},1}a^{\text{D}}_{\mathbf{k}^R,1}\ , \tag{A15}$$

and

$$^{\text{out}}a^{\text{V}}_{\mathbf{K},2}=R_{\text{V},2}a^{\text{V}}_{\mathbf{K}^R,2}+T_{\text{V},2}a^{\text{D}}_{\mathbf{k},2}\ , \tag{A16}$$

$$^{\text{out}}a^{\text{D}}_{\mathbf{k},2}=T_{\text{D},2}a^{\text{V}}_{\mathbf{K},2}+R_{\text{D},2}a^{\text{D}}_{\mathbf{k}^R,2}\ . \tag{A17}$$

As for these modes the Fresnel coefficients are real the same relations hold also for the creation operators $^{\text{out}}a^{\dagger\text{V}}_{\mathbf{K},s}$ and $^{\text{out}}a^{\dagger\text{D}}_{\mathbf{k},s}$.

For the evanescent D modes we have

$$^{\text{out}}a^{\text{D}}_{\mathbf{k},s}=R_{\text{D},s}(\theta^R)a^{\text{D}}_{\mathbf{k}^R,s}\ , \tag{A18}$$

$$^{\text{out}}a^{\dagger\text{D}}_{\mathbf{k},s}=R^{*}_{\text{D},s}(\theta^R)a^{\dagger\text{D}}_{\mathbf{k}^R,s}\ . \tag{A19}$$

The vector potential $\mathbf{A}$ given by Eq. (A8), as well as the other EM field operators, can be equivalently expressed by the outgoing modes and the outgoing operators.

$$\mathbf{A}(\mathbf{r})=\frac{-i}{(2\pi)^3\sqrt{\epsilon_0}}\sum_{s=1,2}\left\{\int_{k_3<0}d_3\mathbf{k}\frac{1}{\sqrt{K}}[^{\text{out}}a^{\text{D}}_{\mathbf{k},s}\,^{\text{out}}\mathcal{E}^{\text{D}}_{\mathbf{k},s}-^{\text{out}}a^{\dagger\text{D}}_{\mathbf{k},s}\,^{\text{out}}\mathcal{E}^{*\text{D}}_{\mathbf{k},s}]\right.$$
$$\left.+\int_{K_3>0}d_3\mathbf{K}\frac{1}{\sqrt{K}}[^{\text{out}}a^{\text{V}}_{\mathbf{K},s}\,^{\text{out}}\mathcal{E}^{\text{V}}_{\mathbf{K},s}-^{\text{out}}a^{\dagger\text{V}}_{\mathbf{K},s}\,^{\text{out}}\mathcal{E}^{*\text{V}}_{\mathbf{K},s}]\right\}\ . \tag{A20}$$

Let us point out that the integration limits are changed according to a new parametrization of the modes and photons.

APPENDIX B

The following matrixes appear in the resolvent functions:

$$\hat{\mathbf{M}}_1=\frac{1}{\pi}\int_0^{2\pi}d\phi\,\hat{\mathbf{e}}\hat{\mathbf{e}}=\begin{bmatrix}1&0&0\\0&1&0\\0&0&0\end{bmatrix}\ , \tag{B1}$$

$$\hat{\mathbf{M}}_2(\alpha)=\frac{1}{\pi}\int_0^{2\pi}d\phi(\hat{\mathbf{p}}\times\hat{\mathbf{e}})(\hat{\mathbf{p}}^{\mathbf{R}}\times\hat{\mathbf{e}})$$
$$=\begin{bmatrix}-\cos^2\alpha&0&0\\0&-\cos^2\alpha&0\\0&0&2\sin^2\alpha\end{bmatrix}\ , \tag{B2}$$

where $\hat{\mathbf{p}}$ can be either $\hat{\mathbf{k}}$ or $\hat{\mathbf{c}}$.

$$\hat{\mathbf{M}}_3(\alpha)=\frac{1}{\pi}\int_0^{2\pi}d\phi(\hat{\mathbf{c}}\times\hat{\mathbf{e}})(\hat{\mathbf{c}}^{*}\times\hat{\mathbf{e}})$$
$$=\begin{bmatrix}n^2\sin^2\alpha-1&0&0\\0&n^2\sin^2\alpha-1&0\\0&0&2n^2\sin^2\alpha\end{bmatrix}\ . \tag{B3}$$

$\hat{\mathbf{M}}_3(\alpha)$ is defined for $n\sin\alpha>1$ only.

APPENDIX C

The following integrals have been used in finding the resolvent function $\mathbf{H}(z)$:

$$\int_0^\infty dK \frac{\cos(aK)}{z^2+K^2} = \frac{\pi}{2z} e^{-az}, \quad \mathrm{Re}z>0$$

$$\int_0^\infty dK \frac{\exp(-aK)}{z^2+K^2} = \frac{1}{z} F(az), \quad \mathrm{Re}z>0$$

where the function

$$F(s) = \mathrm{Ci}(s)\sin(s) - \left[\mathrm{Si}(s) - \frac{\pi}{2}\right]\cos(s) .$$

Ci and Si are the integral cos and sin functions (see [39]).

$$\int_0^\infty dK \frac{\sin(aK)}{z^2+K^2} = \frac{\pi}{2z} G(az), \quad \mathrm{Re}z>0$$

where

$$G(s) = \frac{1}{\pi}[e^{-s}\mathrm{Ei}(s) + e^{s}E_1(s)] ,$$

where Ei and E_1 are the integral exponent functions [39].

The functions $F(z)$ and $G(z)$ which we have just written are multivalued and have a logarithmic branching point at $z=0$. Correct use of these functions requires a right selection of the Riemann surface of those multivalued functions. We note that there is a mirrorlike doubling of these multivalued functions.

All the above integrals, as well as the resolvent function in free space $H_0(z)$ specified before, were calculated under condition $\mathrm{Re}(z)>0$. Defined in this way multivalued functions can be analytically continued into the whole complex z plane. These branches of those functions allow us to determine future evolution of the system that starts from the specified initial data.

Alternatively, we could define the integral functions $H_0^-(z)$, $G^-(z)$, and $F^-(z)$ assuming $\mathrm{Re}(z)<0$ and later by an analytical continuation specify them for the whole z plane. For these branches of the above functions, in the right hand side expressions one should make a replacement $z \to -z$. The above functions would enter the past evolution of the system. They may help to answer a question; what was the past evolution of the system which led to the given state at $t=0$, thus solving the final-value problem. Being interested in future evolution we stay with the branch defined initially for $\mathrm{Re}(z)>0$.

On the imaginary axis of the s plane one has, $s>0$,

$$F(is) = \frac{\pi}{2} e^{-s} - \frac{i}{2}[e^{-s}\mathrm{Ei}(s) + e^{s}E_1(s)] ,$$

$$G(is) = \sin(s) + \frac{2i}{\pi}[\mathrm{Si}(s)\cos(s) - \mathrm{Ci}(s)\sin(s)]$$

so $\mathrm{Re}F(is)$ and $\mathrm{Re}G(is)$, which appear in the decay time calculations, are given by elementary functions.

[1] A. Sommerfeld, Ann. Phys. (Leipzig) **28**, 665 (1909).
[2] A. Sommerfeld, *Partial Differential Equations in Physics* (Academic Press, New York, 1949).
[3] L. B. Felsen and N. Marcuvitz, *Radiation and Scattering of Waves* (Prentice-Hall, Englewood Cliffs, NJ, 1973).
[4] A. Banos, *Dipole Radiation in the Presence of a Conductive Half Space* (Pergamon, New York, 1966).
[5] E. M. Purcell, Phys. Rev. **69**, 681 (1946).
[6] S. Haroche and D. Kleppner, Phys. Today **42** (1), 24 (1989).
[7] K. H. Drexhage, H. Kuhn, and F. P. Schaefer, Ber Bunsenges. Phys. Chem. **72**, 329 (1968).
[8] K. H. Drexhage, Sci. Am. **22**, 108 (1970).
[9] K. H. Drexhage, in *Progress in Optics,* edited by E. Wolf (North-Holland, Amsterdam, 1974), Vol. XII.
[10] H. Morawitz, Phys. Rev. **187**, 1792 (1969).
[11] H. Morawitz and M. R. Philpott, Phys. Rev. B **10**, 4863 (1974).
[12] R. R. Chance, A. Prock, and R. Silbey, J. Chem. Phys. **60**, 2744 (1974).
[13] R. R. Chance, A. Prock, and R. Silbey, Phys. Rev. A **12**, 1448 (1975).
[14] E. A. Hinds, in *Advancs in Atomic, Molecular, and Optical Physics,* edited by D. Bates and B. Bederson (Academic Press, New York, 1991).
[15] V. Sandoghar, C. I. Sukenik, A. Hinds, and S. Haroche, Phys. Rev. Lett. **68**, 3432 (1992).
[16] G. Barton, J. Phys. B **7**, 2134 (1974).
[17] G. S. Agarwal, Phys. Rev. A **12**, 1475 (1975).
[18] G. S. Agarwal, Opt. Commun. **42**, 205 (1982).
[19] J. M. Wylie and J. E. Sipe, Phys. Rev. A **30**, 1185 (1984).
[20] J. M. Wylie and J. E. Sipe, Phys. Rev. A **32**, 2030 (1985).
[21] R. J. Cook and P. W. Milonni, Phys. Rev. A **35**, 5081 (1987).
[22] H. F. Arnoldus and Th.F. George, Phys. Rev. A **37**, 761 (1988).
[23] H. F. Arnoldus and Th.F. George, Phys. Rev. A **43**, 3675 (1991).
[24] F. DeMartini, M. Marocco, P. Mataloni, L. Crescentini, and R. Loudon, Phys. Rev. A **43**, 2480 (1991).
[25] H. Khosravi and R. Loudon, Proc. R. Soc. London, Ser. A **433**, 337 (1991).
[26] G. Björk, S. Machida, Y. Yamamoto, and K. Igeta, Phys. Rev. A **44**, 669 (1991).
[27] R. J. Glauber and M. Lewenstein, Phys. Rev. A **43**, 467 (1991).
[28] E. Yablonovich, T. J. Gmitter, and R. Bhat, Phys. Rev. Lett. **61**, 2546 (1988).
[29] K. Rzążewski and W. Żakowicz, J. Phys. A **9**, 1959 (1976).
[30] K. Rzążewski and W. Żakowicz, J. Math. Phys. **21**, 378 (1980).
[31] C. K. Carniglia, L. Mandel, and K. H. Drexhage, J. Opt. Soc. Am. **62**, 479 (1972).
[32] T. P. Burghardt and N. L. Thompson, Biophys. J. **46**, 730 (1984).
[33] W. Żakowicz, Phys. Rev. A (to be published).
[34] C. K. Carniglia and L. Mandel, Phys. Rev. D **3**, 280 (1971).
[35] I. Białynicki-Birula and J. B. Brojan, Phys. Rev. D **5**, 485 (1972).
[36] H. Rochlin and L. Davidovich, Phys. Rev. A **22**, 2329

(1983).
[37] W. Heitler, *The Quantum Theory of Radiation* (Clarendon Press, Oxford, 1954).
[38] C. Cohen-Tanoudji, J. Dupont-Roc, and G. Grynberg, *Photons and Atoms* (John Wiley & Sons, New York, 1989).
[39] *Handbook of Mathematical Functions,* edited by M. Abramowitz and I. Stegun (Dover, New York, 1970).

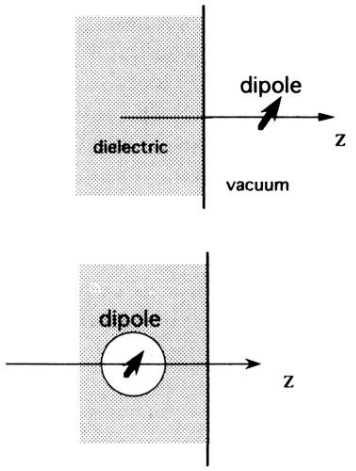

FIG. 1. Oscillator near dielectric-vacuum interface. The oscillator in a dielectric is placed in a microscopic spherical vacuum hole.

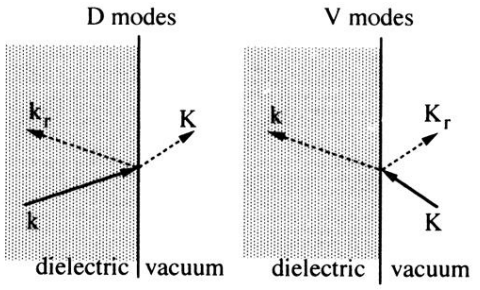

FIG. 6. Carniglia-Mandel dielectric-vacuum modes.

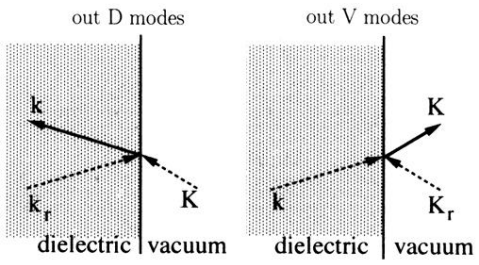

FIG. 7. Outgoing dielectric-vacuum modes.